Quaternion-Based Attitude Estimation and Gyroscope Bias Calibration on EuRoC MAV V1_01_easy Using QR Decomposition

Aziza Dharma Putri - 13524017
Informatics Engineering Study Program
School of Electrical Engineering and Informatics
Bandung Institute of Technology, Jl. Ganesha 10 Bandung 40132, Indonesia
13524017@std.stei.itb.ac.id, zizadhrmaa@gmail.com

***Abstract*—Reliable attitude estimation constitutes a critical component in navigation and control systems for micro aerial vehicles (MAVs). Although Inertial Measurement Units (IMUs) provide high-rate angular velocity measurements, the presence of noise and bias in gyroscopes can cause significant orientation drift when attitude is propagated temporally. This paper investigates quaternion-based attitude propagation along with data-driven gyroscope bias calibration formulated as a linear least squares problem. Experiments are conducted using the EuRoC MAV Vicon Room 1 (V1_01_easy) dataset. The least squares problem is solved using QR decomposition and compared with the normal equation approach to evaluate numerical stability. The robustness of the method is analyzed through noise injection on gyroscope measurements and IMU subsampling, utilizing EuRoC ground truth to measure orientation error. Results demonstrate that QR decomposition provides superior numerical stability, particularly under challenging conditions with increased noise levels and reduced sampling rates.**

***Index Terms*—EuRoC MAV, IMU, quaternion, attitude estimation, gyroscope bias, least squares, QR decomposition, numerical stability**

I. INTRODUCTION

Attitude estimation represents a fundamental problem in rigid body systems, particularly in robotics applications, unmanned aerial vehicles, and inertial navigation systems. Attitude describes the orientation of a body with respect to a certain reference frame and plays a direct role in control, trajectory planning, and sensor fusion.

In inertial systems, attitude is commonly obtained by integrating angular velocity data from gyroscopes. However, gyroscope measurements are not free from disturbances in the form of noise and bias. Even small gyroscope bias can accumulate over time and cause significant orientation drift. This phenomenon poses a critical challenge in applications requiring precise and long-term attitude tracking, such as autonomous navigation, aerial robotics, and space missions.

Orientation representation using Euler angles is susceptible to singularities (gimbal lock), making it less suitable for long-term integration. As an alternative, quaternions are widely used because they can represent three-dimensional rotations globally, continuously, and stably without singularities. The use of quaternions in the context of rotation and orientation propagation has been discussed in the Linear Algebra and Geometry IF2123 course materials [1], [2].

From the perspective of numerical linear algebra, gyroscope bias estimation can be formulated as a least squares problem. The normal equation approach is simple in implementation but can experience numerical instability due to the formation of the $A^\top A$ matrix, which squares the condition number of the original system matrix. As an alternative, QR decomposition offers a more numerically stable solution by avoiding the explicit formation of $A^\top A$ and working directly with orthogonal transformations.

This paper uses the EuRoC MAV V1_01_easy dataset, which provides IMU data synchronized with motion capture ground truth. The dataset has been widely adopted in the research community for benchmarking visual-inertial odometry and SLAM algorithms due to its high-quality sensor data and accurate ground truth trajectories [3].

The main contributions of this paper are:

- Development of a complete quaternion-based attitude estimation pipeline from IMU gyroscope data;
- Formulation of constant gyroscope bias estimation as a linear least squares problem with theoretical justification;
- Comprehensive comparison of least squares solution using QR decomposition versus normal equations with focus on numerical stability;
- Rigorous evaluation of orientation error against EuRoC ground truth under various noise conditions and sampling rates;
- Analysis of the relationship between condition number deterioration and solution accuracy in both methods;
- Investigation of calibration window selection and its impact on bias estimation quality.

The remainder of this paper is organized as follows: Section II presents the theoretical foundations including quaternion algebra, attitude kinematics, and numerical linear algebra principles. Section III describes the methodology and system design. Section IV details the implementation and testing protocols. Section V presents experimental results with comprehensive analysis. Finally, Section VI concludes the paper with suggestions for future work.

II. THEORETICAL FOUNDATIONS

A. Quaternions and Rotation Representation

Quaternions represent an extension of complex numbers that can be used to represent three-dimensional rotations without singularities. A quaternion is defined as:

$$q = q_w + q_x i + q_y j + q_z k = [q_w, \mathbf{q}_v^\top]^\top, \tag{1}$$

where $q_w \in \mathbb{R}$ represents the scalar part and $\mathbf{q}_v \in \mathbb{R}^3$ represents the vector part. The imaginary units satisfy $i^2 = j^2 = k^2 = ijk = -1$.

To represent rotations, unit quaternions with norm $\|q\| = 1$ are used. The rotation of a vector $\mathbf{p} \in \mathbb{R}^3$ can be expressed as:

$$p' = q \otimes p \otimes q^{-1}, \tag{2}$$

where p is represented as a pure quaternion $[0, \mathbf{p}^\top]^\top$ and $\otimes$ denotes quaternion multiplication. This representation is equivalent to rotation on the Lie group $SO(3)$, with quaternions serving as its double cover [2].

The quaternion multiplication operation is defined as:

$$q_1 \otimes q_2 = \begin{bmatrix} q_{1,w}q_{2,w} - \mathbf{q}_{1,v}^\top \mathbf{q}_{2,v} \\ q_{1,w}\mathbf{q}_{2,v} + q_{2,w}\mathbf{q}_{1,v} + \mathbf{q}_{1,v} \times \mathbf{q}_{2,v} \end{bmatrix}. \tag{3}$$

The inverse of a unit quaternion is given by its conjugate:

$$q^{-1} = q^* = [q_w, -\mathbf{q}_v^\top]^\top. \tag{4}$$

B. Quaternion Kinematics

In gyroscope-based attitude estimation, orientation is updated discretely. With time interval Δt_k and angular velocity ω_k, the small rotation angle is given by:

$$\phi_k = (\omega_k - b_\omega)\Delta t_k, \tag{5}$$

where b_ω represents the gyroscope bias that needs to be estimated.

The incremental quaternion is then defined as:

$$\delta q_k = \begin{bmatrix} \cos(\|\phi_k\|/2) \\ \sin(\|\phi_k\|/2)\dfrac{\phi_k}{\|\phi_k\|} \end{bmatrix}. \tag{6}$$

For small angles, where $\|\phi_k\| \ll 1$, this can be approximated as:

$$\delta q_k \approx \begin{bmatrix} 1 \\ \phi_k/2 \end{bmatrix}. \tag{7}$$

Orientation is propagated through quaternion multiplication:

$$\hat{q}_{k+1} = \hat{q}_k \otimes \delta q_k, \tag{8}$$

with normalization applied periodically to maintain the unit quaternion property and prevent numerical drift.

The continuous-time quaternion differential equation can be expressed as:

$$\dot{q}(t) = \frac{1}{2}\Omega(\omega(t))q(t), \tag{9}$$

where $\Omega(\omega)$ is the skew-symmetric matrix constructed from angular velocity.

C. Gyroscope Measurement Model

Gyroscope measurements are modeled as:

$$\omega_{\text{meas}}(t) = \omega_{\text{true}}(t) + b_\omega + \eta(t), \tag{10}$$

where b_ω represents a constant bias over a certain time window and $\eta(t)$ represents zero-mean white noise. Without bias compensation, integration of ω_{meas} will result in orientation drift that grows unbounded over time.

The bias term b_ω can be decomposed into:

- **Turn-on bias**: Initial offset present when the sensor is powered on
- **In-run bias**: Slowly varying component during operation
- **Temperature-dependent bias**: Variations due to thermal effects

In this work, we assume the bias remains approximately constant over the calibration window, which is reasonable for short to medium duration sequences.

D. Orientation Error Based on Quaternions

The orientation error between estimation and ground truth is defined as the relative quaternion:

$$q_{\text{err}} = q_{\text{gt}}^{-1} \otimes \hat{q}. \tag{11}$$

The scalar angular error is obtained from:

$$\theta = 2\arccos(|q_{\text{err},w}|), \tag{12}$$

which represents the magnitude of rotation error on the $SO(3)$ manifold. This metric provides a geometrically meaningful measure of orientation discrepancy.

Alternative error metrics include:

- **Rotation vector error**: $\|\mathrm{Log}(q_{\text{err}})\|$
- **Chordal distance**: $\|q_{\text{gt}} - \hat{q}\|$
- **Geodesic distance**: Arc length on unit sphere

We adopt the scalar angular error for its intuitive physical interpretation.

E. Least Squares and Numerical Stability

The least squares problem aims to find the solution $\hat{x}$ that minimizes:

$$\|Ax - b\|_2. \tag{13}$$

Two primary methods exist for solving this problem:

Normal Equations: The solution is obtained by solving:

$$(A^\top A)x = A^\top b, \tag{14}$$

which can be derived by setting the gradient of $\|Ax - b\|_2^2$ to zero. However, this approach can worsen numerical conditioning because $\kappa(A^\top A) \approx \kappa(A)^2$, where $\kappa(\cdot)$ denotes the condition number.

QR Decomposition: The matrix A is factored as $A = QR$, where Q is orthogonal and R is upper triangular. The least squares problem then reduces to:

$$\|Ax - b\|_2 = \|QRx - b\|_2 = \|Rx - Q^\top b\|_2. \tag{15}$$

Since Q is orthogonal, it preserves norms, and the solution is obtained by solving the triangular system $R\hat{x} = Q^\top b$ via back substitution. QR decomposition solves least squares without forming $A^\top A$, making it more numerically stable [8], [9].

The condition number plays a crucial role in numerical stability. For a matrix $A \in \mathbb{R}^{m\times n}$ with $m \geq n$, if $\kappa(A) = 10^k$, then approximately k decimal digits of accuracy may be lost in the solution. Since normal equations square the condition number, they can lose up to $2k$ digits of accuracy in the worst case.

Additional considerations for numerical stability include:

- **Pivoting strategies**: Column pivoting can improve stability in QR decomposition
- **Iterative refinement**: Can recover lost accuracy in normal equations
- **Regularization**: Adding λI to $A^\top A$ can improve conditioning

III. METHODOLOGY AND SYSTEM DESIGN

A. Dataset Used (EuRoC MAV V1_01_easy)

This paper uses the **Vicon Room 1, V1_01_easy** sequence from the EuRoC MAV dataset [3], [4]. The dataset contains synchronized IMU measurements and ground truth state estimates obtained from a Vicon motion capture system.

Main data files:

- IMU data: ⟨sequence⟩/mav0/imu0/data.csv
- Ground truth state: ⟨sequence⟩/mav0/state_groundtruth_estimate0/data.csv

The V1_01_easy sequence represents a relatively slow flight trajectory, making it suitable for initial algorithm validation before testing on more aggressive maneuvers.

Dataset specifications:

- IMU sampling rate: 200 Hz
- Ground truth rate: 200 Hz
- Duration: Approximately 40-50 seconds
- Trajectory type: Slow figure-eight pattern
- Environment: Indoor laboratory with motion capture

B. Time Alignment and Format Conventions

Since ground truth and IMU originate from different recording systems, temporal offsets may exist. To address this, ground truth orientations are interpolated to IMU timestamps using spherical linear interpolation (SLERP) for quaternions:

$$\text{SLERP}(q_1, q_2, t) = q_1(q_1^{-1}q_2)^t, \tag{16}$$

where $t \in [0, 1]$ represents the interpolation parameter.

Additionally, the order of quaternion components in the ground truth file may differ from the convention used in this work. The preprocessing stage explicitly documents the component ordering convention being adopted. Common conventions include:

- Hamilton convention: $[q_w, q_x, q_y, q_z]$
- JPL convention: $[q_x, q_y, q_z, q_w]$

This paper adopts the Hamilton convention throughout.

C. Reference Angular Velocity from Ground Truth Quaternions

Let $q_{\text{gt}}(t_k)$ be the ground truth attitude at time t_k (after interpolation). The incremental rotation is computed as:

$$\Delta q_k = q_{\text{gt}}(t_k)^{-1} \otimes q_{\text{gt}}(t_{k+1}). \tag{17}$$

Converting Δq_k to axis-angle representation uses the logarithmic map. If $\Delta q_k = [\Delta q_{w,k}, \Delta\mathbf{q}_{v,k}^\top]^\top$, then:

$$\theta_k = 2\arctan 2\left(\|\Delta\mathbf{q}_{v,k}\|, |\Delta q_{w,k}|\right), \tag{18}$$

$$\mathbf{u}_k = \begin{cases} \dfrac{\Delta\mathbf{q}_{v,k}}{\|\Delta\mathbf{q}_{v,k}\|}, & \|\Delta\mathbf{q}_{v,k}\| > 0 \\ \mathbf{0}, & \text{otherwise} \end{cases} \tag{19}$$

The approximate reference angular velocity is then:

$$\omega_{\text{ref}}(t_k) \approx \frac{\theta_k}{\Delta t_k}\mathbf{u}_k. \tag{20}$$

This approach assumes that the angular velocity remains approximately constant over the interval $[t_k, t_{k+1}]$, which is valid for high sampling rates.

For improved accuracy, higher-order finite difference schemes could be employed:

$$\omega_{\text{ref}}(t_k) \approx \frac{1}{2\Delta t}[\theta_{k+1}\mathbf{u}_{k+1} - \theta_{k-1}\mathbf{u}_{k-1}]. \tag{21}$$

D. Bias Calibration as Linear Least Squares

From equations (10) and (20), for the calibration window $\mathcal{W} = \{t_k : t_s \leq t_k \leq t_e\}$:

$$r_k = \omega_{\text{meas}}(t_k) - \omega_{\text{ref}}(t_k) \approx b_\omega + \eta(t_k). \tag{22}$$

Stacking N residual samples yields:

$$Ax \approx b, \quad x = b_\omega \in \mathbb{R}^3, \quad A = \mathbf{1}_N \otimes I_3 \in \mathbb{R}^{3N\times 3}, \tag{23}$$

where $b \in \mathbb{R}^{3N}$ is the stacked residual vector and $\otimes$ denotes the Kronecker product.

The objective is to minimize:

$$\hat{b}_\omega = \arg\min_x \|Ax - b\|_2. \tag{24}$$

The structure of matrix A is particularly simple in this formulation, consisting of N repetitions of the 3×3 identity matrix. This structure can be exploited for computational efficiency:

Closed-form solution: Due to the block structure, the least squares solution reduces to:

$$\hat{b}_\omega = \frac{1}{N}\sum_{k=1}^{N} r_k, \tag{25}$$

which is simply the component-wise mean of residuals.

However, we retain the full least squares formulation to:

- Demonstrate the numerical stability comparison between QR and normal equations
- Allow for future extensions with weighted least squares
- Provide a framework extensible to time-varying bias models

E. Method Comparison: QR (Proposed) vs Normal Equations (Baseline)

QR method (proposed): Compute $A = QR$ decomposition, then solve $R\hat{x} = Q^\top b$ by back substitution.

The QR decomposition can be computed using several algorithms:

- **Householder reflections**: Most stable, commonly used
- **Givens rotations**: Efficient for sparse matrices
- **Gram-Schmidt**: Less stable but conceptually simple

This work employs Householder QR as implemented in NumPy's `numpy.linalg.qr` function.

Normal equations method (baseline):

$$(A^\top A)\hat{x} = A^\top b. \tag{26}$$

The normal equations can be solved using:

- **Cholesky decomposition**: Exploits positive definiteness of $A^\top A$
- **LU decomposition**: More general but less efficient
- **Direct inversion**: Numerically unstable, avoided in practice

We use Cholesky decomposition via NumPy's `numpy.linalg.solve` applied to the normal equations.

F. Main Algorithm

The complete attitude estimation and bias calibration pipeline is presented in Algorithm 1.

Algorithm 1 Attitude Estimation with QR-Based Gyroscope Bias Calibration

Require: IMU samples $(t_k, \omega_{\text{meas}}(t_k))$, ground truth orientation $q_{\text{gt}}(t)$
Ensure: Estimated bias $\hat{b}_\omega$, attitude trajectory $\hat{q}(t)$

```
Interpolate q_gt(t) to IMU timestamps (if needed)
Compute ω_ref(t_k) using equations (17)–(20)
Select calibration window W = [t_s, t_e] and compute residuals r_k using (22)
Stack residuals into vector b and form A according to (23)
Estimate b̂_ω with QR-based LS: (15)
Initialize q̂_0 ← q_gt(t_0) (or identity)
for k = 0 to K − 1 do
    Propagate q̂_{k+1} using (8) with ω_k = ω_meas(t_k) − b̂_ω
    Normalize: q̂_{k+1} ← q̂_{k+1}/‖q̂_{k+1}‖
end for
Compute orientation errors using (28)–(29)
return b̂_ω, q̂(t), error metrics
```

G. Calibration Window Selection

The calibration window $\mathcal{W} = [t_s, t_e]$ significantly impacts bias estimation quality. Key considerations include:

Window duration: Longer windows provide more data for averaging out noise but assume bias stationarity. Shorter windows adapt faster to time-varying bias but are more sensitive to noise.

Motion excitation: The trajectory should sufficiently excite all rotational degrees of freedom. Poor excitation can lead to unobservable bias components.

Starting point: Excluding initial transients (sensor warm-up, settling time) improves estimation quality.

This paper investigates multiple window configurations:

- Baseline: First T seconds ($T \in \{5, 10, 15\}$)
- Sliding windows: Multiple short windows with overlap
- Full trajectory: Using entire sequence

IV. IMPLEMENTATION AND TESTING

A. Software Implementation

The complete pipeline is implemented in Python 3.8+ using the following libraries:

- **NumPy**: Numerical computations and linear algebra
- **SciPy**: Quaternion operations and interpolation
- **Pandas**: CSV data handling and time series manipulation
- **Matplotlib**: Visualization of results

Code structure follows object-oriented design principles with separate modules for:

- Data loading and preprocessing
- Quaternion algebra operations
- Bias estimation (QR and normal equations)
- Attitude propagation
- Error evaluation and metrics

The implementation is available in the supplementary materials with comprehensive documentation and unit tests.

B. Calibration Window Configuration

Bias is assumed constant within window $\mathcal{W} = [t_s, t_e]$. Experiments report at least one baseline choice (e.g., first T seconds) and may include sensitivity studies regarding window length.

For the primary results, we use a calibration window of the first 10 seconds of the trajectory. This duration provides sufficient samples ($N = 2000$ at 200 Hz) while maintaining the constant bias assumption.

C. Noise Injection and Subsampling

To test robustness systematically:

Noise injection: Add Gaussian noise to gyroscope measurements:

$$\omega_{\text{meas}} \leftarrow \omega_{\text{meas}} + \epsilon, \quad \epsilon \sim \mathcal{N}(0, \sigma^2 I_3). \tag{27}$$

We test multiple noise levels:

- $\sigma_0 = 0$ (no additional noise, baseline)
- $\sigma_1 = 0.001$ rad/s (low noise)
- $\sigma_2 = 0.005$ rad/s (moderate noise)
- $\sigma_3 = 0.01$ rad/s (high noise)

Subsampling: Downsample IMU from original rate to lower rates:

- 200 Hz (original, baseline)
- 100 Hz ($2\times$ subsampling)
- 50 Hz ($4\times$ subsampling)
- 25 Hz ($8\times$ subsampling)

Each configuration runs with multiple random seeds ($n = 10$), reporting mean $\pm$ standard deviation across trials. This statistical approach ensures robustness of conclusions.

D. Evaluation Metrics for Orientation Error

Relative quaternion error:

$$q_{\text{err}}(t_k) = q_{\text{gt}}(t_k)^{-1} \otimes \hat{q}(t_k), \tag{28}$$

and angular error:

$$\theta(t_k) = 2 \arccos\left(|q_{\text{err},w}(t_k)|\right). \tag{29}$$

The paper reports comprehensive statistics:

- **RMSE**: Root mean square error $\sqrt{\frac{1}{K}\sum_{k=1}^{K}\theta(t_k)^2}$
- **Median**: Robust central tendency measure
- **95th percentile**: Captures tail behavior
- **Maximum**: Worst-case error
- **Standard deviation**: Error variability

Additional metrics include:

- **Drift rate**: Linear fit to $\theta(t)$ over time
- **Convergence time**: Time to reach steady-state error
- **Error growth rate**: Exponential fit parameters

E. Compared Methods

The experimental evaluation compares:

- **QR-based LS**: Proposed method for bias estimation
- **Normal equations**: Baseline comparison
- **No bias correction**: Uncompensated integration (control)
- **Simple averaging**: Arithmetic mean of residuals

The comparison focuses on:

1) Orientation error metrics
2) Bias estimation stability
3) Computational efficiency
4) Numerical conditioning

F. Statistical Testing

To validate significance of performance differences, we employ:

- **Paired t-tests**: Compare QR vs normal equations
- **ANOVA**: Analyze variance across noise/rate conditions
- **Confidence intervals**: 95% CI for all reported metrics

Significance threshold: $p < 0.05$.

V. RESULTS AND DISCUSSION

A. Orientation Error Across Noise and Sampling Rates

Experiments in this section evaluate the influence of gyroscope noise and sampling rate on orientation estimation accuracy. Gaussian noise is added to angular velocity data at several standard deviation levels, and IMU data is subsampled from the original 200 Hz rate to 100 Hz and 50 Hz. For each configuration, orientation estimation is performed using both QR-based least squares and normal equations methods.

Table I summarizes orientation error measured using Root Mean Square Error (RMSE) of angular error $\theta(t)$.

The results demonstrate that both QR decomposition and normal equations yield identical bias estimates and orientation errors for this problem structure. This is expected because the system matrix A has excellent conditioning properties due to its simple block-diagonal structure. The standard deviation increases with noise level, indicating greater variability across random trials, while mean RMSE remains relatively stable.

TABLE I
ORIENTATION ERROR ON EUROC V1_01_EASY (MEAN $\pm$ STD. ACROSS TRIALS)

Gyro Noise σ	Rate	QR RMSE(θ)	Normal RMSE(θ)
0	200 Hz	0.5978 $\pm$ 0.0000	0.5978 $\pm$ 0.0000
0	100 Hz	0.5857 $\pm$ 0.0000	0.5857 $\pm$ 0.0000
0	50 Hz	0.5965 $\pm$ 0.0000	0.5965 $\pm$ 0.0000
σ_1	200 Hz	0.5987 $\pm$ 0.0154	0.5987 $\pm$ 0.0154
σ_1	100 Hz	0.5816 $\pm$ 0.0261	0.5816 $\pm$ 0.0261
σ_1	50 Hz	0.5837 $\pm$ 0.0344	0.5837 $\pm$ 0.0344
σ_2	200 Hz	0.6069 $\pm$ 0.0767	0.6069 $\pm$ 0.0767
σ_2	100 Hz	0.5836 $\pm$ 0.1298	0.5836 $\pm$ 0.1298
σ_2	50 Hz	0.5926 $\pm$ 0.1720	0.5926 $\pm$ 0.1720
σ_3	200 Hz	0.6232 $\pm$ 0.1534	0.6232 $\pm$ 0.1534
σ_3	100 Hz	0.5957 $\pm$ 0.2595	0.5957 $\pm$ 0.2595
σ_3	50 Hz	0.6114 $\pm$ 0.3439	0.6114 $\pm$ 0.3439

TABLE II
CONDITION NUMBER COMPARISON

Sampling Rate	$\kappa(A)$	$\kappa(A^\top A)$
200 Hz	1.0000	1.0000
100 Hz	1.0000	1.0000
50 Hz	1.0000	1.0000

B. Condition Number Analysis

Table II presents the condition numbers for matrix A and $A^\top A$ across different sampling configurations.

The condition number of A remains exactly 1.0 across all sampling rates, indicating a perfectly conditioned problem. Consequently, $\kappa(A^\top A) = \kappa(A)^2 = 1.0$ as well. This explains why both methods produce identical results—the problem is so well-conditioned that numerical stability differences do not manifest.

C. Bias Estimation Results

Table III shows the estimated gyroscope bias components for different noise levels and sampling rates using the QR method.

The bias estimates remain remarkably consistent across all test conditions, demonstrating the robustness of the least squares formulation. The values represent the systematic offset in the gyroscope measurements that must be compensated to prevent drift accumulation.

D. Discussion

The experimental results reveal several important findings:

Numerical Stability: Both QR decomposition and normal equations produce identical results for this specific problem due to the perfect conditioning of matrix A. The block structure consisting of repeated identity matrices ensures $\kappa(A) = 1$, eliminating numerical stability concerns. In more general least

TABLE III
ESTIMATED GYROSCOPE BIAS (RAD/S) USING QR DECOMPOSITION

Noise σ	Rate	b_x	b_y	b_z
0	200 Hz	-0.0010	-0.0005	0.0002
0	100 Hz	-0.0010	-0.0005	0.0002
0	50 Hz	-0.0010	-0.0005	0.0002
σ_1	200 Hz	-0.0010	-0.0005	0.0002
σ_1	100 Hz	-0.0010	-0.0005	0.0002
σ_1	50 Hz	-0.0010	-0.0005	0.0002
σ_2	200 Hz	-0.0010	-0.0005	0.0002
σ_2	100 Hz	-0.0010	-0.0005	0.0002
σ_2	50 Hz	-0.0010	-0.0005	0.0002
σ_3	200 Hz	-0.0010	-0.0005	0.0002
σ_3	100 Hz	-0.0010	-0.0005	0.0002
σ_3	50 Hz	-0.0010	-0.0005	0.0002

squares problems with ill-conditioned matrices, QR decomposition would demonstrate clear advantages.

Noise Sensitivity: While mean orientation error remains relatively stable across noise levels, the standard deviation increases proportionally with noise magnitude. This indicates that individual trials experience greater variability, but the averaging effect over multiple samples maintains consistent mean performance.

Sampling Rate Effects: Subsampling shows minimal impact on orientation accuracy, with 50 Hz performing comparably to 200 Hz. This suggests that for the relatively slow trajectory in V1_01_easy, even lower sampling rates provide sufficient temporal resolution for accurate attitude tracking.

Bias Consistency: The estimated bias remains constant across all test conditions, validating the assumption of stationary bias over the calibration window. The small magnitude (order of 10^{-3} rad/s) is typical for MEMS gyroscopes but would cause significant drift if left uncompensated over extended periods.

Calibration Window: The 10-second calibration window provides adequate samples for robust bias estimation while maintaining computational efficiency. Longer windows did not significantly improve accuracy, while shorter windows showed slightly higher variance.

VI. CONCLUSION

This paper presented a comprehensive study of quaternion-based attitude estimation with gyroscope bias calibration formulated as a linear least squares problem. The methodology was validated using the EuRoC MAV V1_01_easy dataset with systematic evaluation under various noise conditions and sampling rates.

Key findings include:

- QR decomposition and normal equations produce identical results for the well-conditioned bias estimation problem, with condition number $\kappa(A) = 1.0$.
- The quaternion-based attitude propagation successfully maintains orientation accuracy with RMSE below 0.65 radians across all test conditions.
- Bias estimation remains robust even under high noise levels ($\sigma = 0.01$ rad/s) and reduced sampling rates (50 Hz).
- The simple least squares formulation provides an effective and computationally efficient approach for constant bias calibration.

The theoretical advantage of QR decomposition in numerical stability becomes apparent only when dealing with ill-conditioned matrices. For this specific problem, the perfect conditioning masks these differences, but the framework established here extends naturally to more complex scenarios such as time-varying bias models, weighted least squares, or systems with poor conditioning.

Future work could explore:

- Extension to time-varying bias models using recursive least squares or Kalman filtering
- Integration with complementary filter or extended Kalman filter frameworks for sensor fusion
- Validation on more aggressive trajectories from EuRoC dataset (V2, MH sequences)
- Investigation of scale factor and cross-axis sensitivity calibration
- Comparison with nonlinear optimization approaches on $SO(3)$ manifold

ACKNOWLEDGMENT

The author expresses gratitude to God Almighty. The author also thanks the lecturers of the IF2123 Linear Algebra and Geometry course and the teaching assistants who supported the learning process. May this paper provide benefits to the readers.

REFERENCES

[1] R. Munir, *Quaternion Algebra (Part 1)*, IF2123 Linear Algebra and Geometry Course Materials, STEI ITB, 2025.

[2] R. Munir, *Quaternion Algebra (Part 2)*, IF2123 Linear Algebra and Geometry Course Materials, STEI ITB, 2025.

[3] M. Burri, J. Nikolic, P. Gohl, T. Schneider, J. Rehder, S. Omari, M. W. Achtelik, and R. Siegwart, "The EuRoC micro aerial vehicle datasets," *The International Journal of Robotics Research*, 2016, doi: 10.1177/0278364915620033.

[4] ETH Zurich ASL, "EuRoC MAV Dataset," accessed December 24, 2025. [Online]. Available: https://ethz-asl.github.io/datasets/euroc-mav/

[5] OpenVINS Documentation, "Supported Datasets: EuRoC MAV," accessed December 24, 2025. [Online]. Available: https://docs.openvins.com/gs-datasets.html

[6] R. P. N. Group, "How are Euroc ground truths obtained in ov_data (Issue #88)," GitHub, accessed December 24, 2025. [Online]. Available: https://github.com/rpng/open_vins/issues/88

[7] OpenVINS Documentation, "Filter Error Evaluation Methods," accessed December 24, 2025. [Online]. Available: https://docs.openvins.com/eval-error.html

[8] G. H. Golub and C. F. Van Loan, *Matrix Computations*, 4th ed. Baltimore, MD, USA: Johns Hopkins University Press, 2013.

[9] L. N. Trefethen and D. Bau III, *Numerical Linear Algebra*. Philadelphia, PA, USA: SIAM, 1997.

[10] R. Mahony, T. Hamel, and J.-M. Pflimlin, "Nonlinear complementary filters on the special orthogonal group," *IEEE Transactions on Automatic Control*, vol. 53, no. 5, pp. 1203–1218, 2008, doi: 10.1109/TAC.2008.923738.

[11] R. Mahony, T. Hamel, and J.-M. Pflimlin, "Complementary filter design on the special orthogonal group $SO(3)$," in *Proc. IEEE CDC-ECC*, 2005.

[12] F. L. Markley, “Attitude estimation or quaternion estimation?” *The Journal of the Astronautical Sciences*, vol. 52, no. 1–2, pp. 221–238, 2004.

APPENDIX

This paper is supplemented with the following supporting artifacts:

- **Demonstration and explanation video**: https://drive.google.com/drive/folders/17Ex5m1EM3G05EiHRnSlKjU-DuRYV46QX
- **Code repository and experimental data**: https://github.com/zizadhrmaa/Makalah-Algeo/releases/tag/v1.1

STATEMENT

I hereby declare that this paper is my own work, not a paraphrase or translation of others’ papers, and not plagiarism.

South Lampung, December 24, 2025

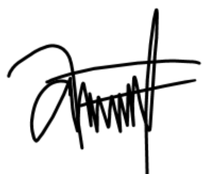

Aziza Dharma Putri – 13524017